

## PREDICTIVE REVIEW

# Testing for changes in rate of evolution and position of the climatic niche of clades

Silvia CASTIGLIONE *Department of Earth Sciences, Environment and Resources, University of Naples Federico II, 80138 Naples, Italy. Email: [silvia.castiglione@unina.it](mailto:silvia.castiglione@unina.it)*

Alessandro MONDANARO *Department of Earth Sciences, University of Florence, 50121 Florence, Italy. Email: [alessandro.mondanaro@unifi.it](mailto:alessandro.mondanaro@unifi.it)*


Mirko DI FEBBRARO *Department of Biosciences and Territory, University of Molise, C. da Fonte Lappone, 15, 86090 Pesche, IS, Italy. Email: [mirkodifebbraro@gmail.com](mailto:mirkodifebbraro@gmail.com)*

Marina MELCHIONNA *Department of Earth Sciences, Environment and Resources, University of Naples Federico II, 80138 Naples, Italy. Email: [marina.melchionna@unina.it](mailto:marina.melchionna@unina.it)*

Carmela SERIO *Research Centre in Evolutionary Anthropology and Palaeoecology, School of Biological and Environmental Sciences, Liverpool John Moores University, Liverpool, UK. Email: [c.serio@2019.ljmu.ac.uk](mailto:c.serio@2019.ljmu.ac.uk)*

Giorgia GIRARDI *Department of Earth Sciences, Environment and Resources, University of Naples Federico II, 80138 Naples, Italy. Email: [girardi.giorgia.gg@gmail.com](mailto:girardi.giorgia.gg@gmail.com)*

Arianna Morena BELFIORE *Department of Earth Sciences, Environment and Resources, University of Naples Federico II, 80138 Naples, Italy. Email: [arianna.m.belfiore@gmail.com](mailto:arianna.m.belfiore@gmail.com)*

Pasquale RAIA  *Department of Earth Sciences, Environment and Resources, University of Naples Federico II, 80138 Naples, Italy. Email: [pasquale.raia@unina.it](mailto:pasquale.raia@unina.it)*

### Keywords

climatic niche evolution, global, niche drift, niche shift, `phylo.niche.shift`, primates, R<sub>R</sub>phylo

### \*Correspondence

Received: 6 July 2022

Accepted: 10 August 2022

Editor: DR

doi: 10.1111/mam.12303

## ABSTRACT

1. There is solid recognition that phylogenetic effects must be acknowledged to appreciate climatic niche variability among species clades properly. Yet, most currently available methods either work at the intra-specific level (hence they ignore phylogeny) or rely on the Brownian motion model of evolution to estimate phylogenetic effects on climatic niche variation. The Brownian motion model may be inappropriate to describe niche evolution in several cases, and even a significant phylogenetic signal in climatic variables does not indicate that the effect of shared ancestry was relevant to niche evolution.
2. We introduce a new phylogenetic comparative method which describes significant changes in the width and position of the climatic niche at the inter-specific (clade) level, while making no *a priori* assumption about how niche evolution took place.
3. We devised the R function `phylo.niche.shift` to estimate whether the climatic niches of individual clades in the tree are either wider or narrower than expected, and whether the niche occupies unexpected climates. We tested `phylo.niche.shift` on realistic virtual species' distribution patterns applied to a phylogeny of 365 extant primate species.
4. We demonstrate via simulations that the new method is fast and accurate under widely different climatic niche evolution scenarios. `phylo.niche.shift` showed that the capuchin monkeys and langurs occupy much wider, and prosimian much narrower, climatic niche space than expected by their phylogenetic positions.
5. `phylo.niche.shift` may help to improve research on niche evolution by allowing researchers to test specific hypotheses on the factors affecting clades' realised niche width and position, and the potential effects of climate change on species' distributions.

## INTRODUCTION

The climatic niche of a species is defined by the set of temperature and precipitation regimes it experiences (Holt & Gaines 1992). Although the climatic niche is not a phenotypic trait *per se*, climatic preferences depend directly on the species' physiology and lifestyle (e.g. thermal tolerance limits, dietary preferences, body size), so that the evolution of climatic niches can be studied as if they were phenotypes (Holt & Gaines 1992, Rolland et al. 2018). Starting from this broad assumption, several investigations aimed to evaluate the importance of phylogenetic effects vs. contingency (e.g. competition, local adaptation, human disturbance) at determining the distribution of species (Freckleton & Jetz 2009, Corro et al. 2021), or whether climatic niche variability correlates with species diversity (Kozak & Wiens 2010, Rolland & Salamin 2016). Many studies apply the calculation of the phylogenetic signal (Blomberg et al. 2003) in niche variability as a measure of the degree of phenotypic resemblance between species. In the context of climatic niche evolution, high phylogenetic signal would indicate that phylogenetically close species live under more similar climates than distant species, provided the Brownian motion model (BM) is an appropriate descriptor of climatic niche evolution (Freckleton 2009, Kamilar & Cooper 2013, Boucher et al. 2014). Studies consistently indicate a generally weak yet irregular phylogenetic signal in climatic variables (Song et al. 2016, Perez & Feeley 2021); that the upper (warm) thermal tolerance limit is more phylogenetically structured than lower (cold) limit (Diamond & Chick 2018, Lancaster & Humphreys 2020, Perez & Feeley 2021); and that niche breadth correlates with both geographic range size and diversity (Kozak & Wiens 2010, Rolland & Salamin 2016).

Although it is widely used to infer the imprint of shared ancestry on climatic niche evolution, the phylogenetic signal has several limitations. It ignores potential differences between clades in the rate of climatic niche evolution, and describes a pattern rather than a process, meaning that high phylogenetic signal may derive from spatial proximity alone, with no effect of shared ancestry (Freckleton & Jetz 2009). Still, geologically rapid changes in the position of the climatic niche occupied by a clade may result from the emergence of key innovations, dispersals, or changes in the competition regimes that allow for the successful colonisation of previously unexplored habitats (Lancaster & Humphreys 2020). For instance, species belonging to clades distributed at low latitudes are often reported to exploit narrower climatic niches than temperate species clades, suggesting a slower rate of climatic niche evolution in the Tropics (Kozak & Wiens 2010, Rolland et al. 2018). Middle Pleistocene human species were shown to deviate significantly from their ancestors' habitual climatic niche

thanks to cultural innovation (Mondanaro et al. 2020). Panicoideae grasses (e.g. maize, switchgrass) expanded their niches to colonise regions with higher growing season temperatures by exploiting the C4 photosynthetic pathway (Aagesen et al. 2016). Simulation experiments show that latitudinal gradients in niche breadth may occur even without any change in the fundamental species' niche (Saupe et al. 2019), which suggests that the rate of climatic niche evolution and its position should be investigated together.

We devised a method, embodied in the R function `phylo.niche.shift`, which locates major changes in the rate of evolution and in the position of the climatic niche of clades contained within a phylogenetic tree. The method builds on phylogenetic ridge regression as implemented in the `RRphylo` R function (Castiglione et al. 2018). Contrary to BM, `RRphylo` does not assume a single rate of evolution operating through the phylogeny, or that trait (here bioclimatic variables) means should not change over evolutionary time. By using realistic species' distribution patterns, we demonstrate via simulations that `phylo.niche.shift` is especially powerful at pursuing both goals under widely different models of climatic niche evolution. We further applied the method to a phylogeny of 365 extant primate species.

## METHODS

### Simulating virtual species' distributions

Our aim was to test `phylo.niche.shift` on a realistic representation of climatic niche evolution on phylogenetic trees, covering different situations, from negligible to important climatic niche similarity within the clades, while reproducing genuine macroecological patterns of species' distribution on Earth.

We started by locating, on continental Eurasia (the sampling area ranges from  $-20^{\circ}$  to  $180^{\circ}$  longitude, and from  $0^{\circ}$  to  $90^{\circ}$  latitude), a number of virtual species, randomly chosen between 100 and 200. The species are given a certain number of geographic occurrences each, drawn from a negative exponential distribution with rate parameter  $\lambda = 0.1$ , and bound between 100 and 5 occurrences. This way, a few species will be abundant whereas the majority will be rare, in keeping with the well-known shape of the species' abundance-frequency distribution (Gaston & Blackburn 2007). For each species, its first occurrence is randomly placed in Eurasia. A square mask ranging from  $10^6$  to  $1.1 \times 10^7$  square metres is centred around this first occurrence, setting the size of the mask to be proportional to the total number of occurrences (imposing a correlation coefficient between the number of occurrences and the size of the mask  $r = 0.8$ ). All

other occurrences are then randomly placed within the mask.

After all occurrences for all species are located, they are ‘compressed’ towards the equator by applying an exponential transformation with  $\lambda = 0.8$  to the occurrences’ latitude, so that the whole set of species mimics the latitudinal diversity gradient (Gaston & Blackburn 2007). Finally, the occurrences falling outside the landmass of Eurasia are discarded. For each species, we calculated the area of the minimum convex polygon enclosing its occurrences to represent the species’ geographic range size.

At the geographic location of each individual occurrence, we extracted 19 bioclimatic variables values from the Worldclim database (WorldClim version 2.1; Fick & Hijmans 2017) with the native 5-min spatial resolution. To avoid potential problems of multicollinearity, the full set of 19 bioclimatic variables was reduced considering a variance inflation factor  $\leq 5$  (Zuur et al. 2010; see Table 1 for the variables that were selected).

### Simulating different scenarios of climatic evolution on the tree

For each species, we calculated the mean of each variable over all its occurrences to create a bioclimatic vector representing the ‘average’ realised climatic conditions experienced by the species. Then, we constructed three different hypothetical phylogenetic trees by means of hierarchical clustering, using the angle  $\phi$  between bioclimatic vectors (which is equivalent to Pearson’s correlation coefficient) as the distance metric to guide the clustering algorithm. The trees represent three abstract, widely different scenarios of climatic niche evolution:

1. Anticlimatic Evolution (AE). Under AE, phylogenetic proximity is determined by the difference  $90 - \phi$ . Since only few bioclimatic variables (e.g. BIO6, minimum temperature of coldest month) can attain negative values, angles  $> 90^\circ$  (which would represent negative correlation

coefficients) are inappropriate, and were in fact never produced in the simulations. By clustering species via their climatic dissimilarity, under AE, each clade in the tree will have roughly equal chance to include climatically distant species (Fig. 1a). Therefore, the clades in the tree will be formed by species with widely differing climatic preferences and evolve at similar rates of climatic niche change. The phylogenetic signal in climatic variables is expected to be weak.

2. Random Climatic Evolution (RCE). Under RCE, species’ phylogenetic proximity is disconnected from climatic proximity (Boucher et al. 2014). To produce RCE, we first computed the angle  $\phi$  between any pair of species’ bioclimatic vectors. Then, we arbitrarily substituted  $\phi$  with a new value  $\phi_1$  sampled between  $\phi$  and  $90^\circ$  to feed the agglomeration algorithm in hierarchical clustering by using the ‘unweighted pair group method with arithmetic mean’. This way, any signal of climatic resemblance between species is weakened randomly during the tree construction process (Fig. 1b), resulting in the lowest phylogenetic signal of any scenario.

3. Climate-driven evolution (CDE). Under CDE, climatic proximity (that is  $\phi$ ) is used to guide the agglomeration algorithm. Therefore, most clades in the tree will be bound to include species with strongly similar climatic preferences, so that climatic variability represents a strong determinant of species’ geographic distribution (Fig. 1c). The phylogenetic signal is expected to be large, and climatic preferences will be apportioned between, rather than within, clades, generating presumably large evolutionary rate differences between them.

We ran each scenario 1000 times. At each iteration, we first tested the existence of the latitudinal diversity gradient. To this aim, we partitioned all species’ occurrences over consecutive,  $5^\circ$  wide latitudinal bands poleward, and counted the number of species present with at least one occurrence in each band. Then, we regressed species richness per band against the mean latitude of

**Table 1.** A real-case representation of the transformations applied to simulate climatic niche evolution rate shifts to specific clades in the tree. Variable values represent the range of values sampled by the species belonging to the selected clade, pooled together. The bioclimatic variables are from the Worldclim database (WorldClim version 2.1; Fick & Hijmans 2017)

	Temperature				Precipitation			
	Mean diurnal range	Isothermality	Wettest quarter	Driest quarter	Driest month	Seasonality	Warmest quarter	Coldest quarter
	BIO2	BIO3	BIO8	BIO9	BIO14	BIO15	BIO18	BIO19
$y_0$	9.025	28.852	11.874	-4.518	0	50.92	4.328	9.488
	15.717	61.136	29.078	26.885	18.575	128.305	587.316	127.374
$y_{plus}$	6.89	20.105	6.545	-16.09	-2.146	28.658	-70.026	-11.691
	16.929	68.53	32.352	31.014	25.717	144.736	804.455	165.138
$y_{minus}$	10.434	34.626	15.39	3.119	1.416	65.612	53.402	23.465
	14.918	56.255	26.917	24.159	13.861	117.46	444.004	102.449

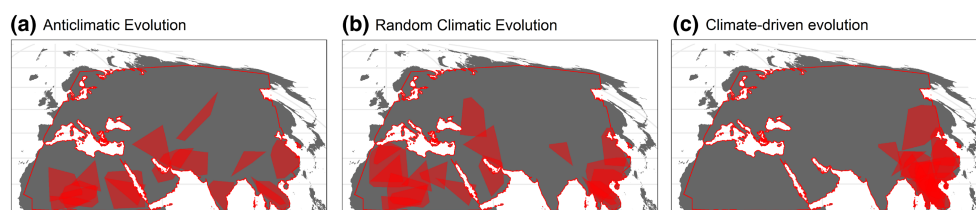


**Fig. 1.** The three different scenarios of species' distributions within clades, representing evolution proceeding according to anticlimatic (a); random (b); or climate-driven (c) preferences in climatic conditions across species.

all the occurrences within each band. We further tested for the existence of the desired positive relationship between geographical range size and latitude (Gutiérrez-Pesquera et al. 2016). We regressed species' range sizes against the mean latitude of the species' occurrences. Both negative and significant diversity-latitude and positive and significant range size-latitude relationships are expected to occur in the data to prove that the simulations were based on realistic species' distribution patterns.

### The `phylo.niche.shift` algorithm for rate shifts

`phylo.niche.shift` calculates the evolutionary rate for each branch in the phylogeny, according to phylogenetic ridge regression as implemented in the `RRphylo` function, embedded in the namesake R package (Castiglione et al. 2018). A function linked to `RRphylo`, `search.shift`, still part of the `RRphylo` toolkit, is called from within `phylo.niche.shift` to locate on the tree shifts in the absolute evolutionary rates by using a randomisation procedure (Castiglione et al. 2018). A significant shift as attached to a particular clade in the phylogeny indicates that clade has more or less climatic variability than expected from its phylogenetic position. `search.shift` allows researchers to test for the existence of the rate shifts in climatic niche evolution either automatically, or by indicating specific clades to be tested.

### Simulating rate shifts as applied to a specific clade

To simulate a rate shift in climatic niche evolution as applied to a particular clade in the tree, we started identifying all the subtrees in the phylogeny  $CC_{can}$  including no less than one-tenth and no more than one half of the tree tips. A clade  $CC_{sel}$  was randomly selected among  $CC_{can}$ . The trace of the evolutionary rate matrix (whose diagonal elements indicate the rate of evolution for individual climatic variables; Revell & Harmon 2008) of  $CC_{sel}$  was computed to represent a measure of its

'multivariate' rate of climatic niche evolution. An  $xs$  scalar was used to transform each bioclimatic variable for each species belonging to  $CC_{sel}$ , according to the equation:

$$xs * y - (xs - 1) * \bar{y}$$

where  $y$  is the bioclimatic variable, and  $\bar{y}$  is its mean computed over the  $CC_{sel}$  species. For  $xs > 1$  the range of the bioclimatic variable values realised by  $CC_{sel}$  species will increase, simulating a faster rate of climatic niche evolution, and the other way around at  $xs < 1$ , whereas the variables mean will not change. Table 1 depicts the actual effect of applying a relatively large  $xs$  ( $xs$  is bound in between  $-2$  and  $2$  in the simulations) on the original range of  $y_0$  values for each bioclimatic variable of the species belonging to  $CC_{sel}$ , either simulating an increase in the rate (with  $xs = 1.5$ ,  $y_{plus}$  in Table 1) or its inverse ( $xs = 0.67$ ,  $y_{minus}$  in Table 1).

Although some variables occasionally take unrealistic values (e.g. negative precipitation values in Table 1), our goal was to simulate feasible and proportionally small contractions (or increases) in climatic variability within the selected clade, which is well represented by the potential range of  $xs$  values we designated. To account for rate heterogeneity and skewed distribution of rates among  $CC_{can}$ , we transformed  $xs$  to a metric *effect* so that at *effect* = 1,  $CC_{sel}$  evolves at the same rate as the rest of the tree, and with *effect*  $\neq$  1, the impact of rate transformation is symmetric for rate decreases and increases (see Appendix S1). We further calculated Type I error at *effect* = 1.

### The `phylo.niche.shift` algorithm for niche drifts

To test for potential drift (a change in the position of the climatic niche of the clade) for each  $CC_{can}$ , `phylo.niche.shift` computes the Mahalanobis distance between the bioclimatic vectors of the species belonging to the focal clade and the mean bioclimatic values of all the other species in the tree as well as their covariance. The Mahalanobis distance is a *scale-invariant*



generalisation of the Euclidean distance for correlated variables. Therefore, it is best suited to measure the 'distance' between each  $CC_{can}$  and the rest of the tree. In `phylo.niche.shift`, a family of 100 random Mahalanobis distances is created by extracting from the tree bioclimatic vectors a random subset of  $n$  species for any clade of size  $n$  within  $CC_{can}$ , and computing the Mahalanobis distance between this set of  $n$  species and the rest of the tree. Significance is assessed by comparing the real Mahalanobis distance to the random distances and accepting as significant a real distance outside the range of random distances.

For any clade found to drift  $CC_{drift}$  (or for a clade specified by the user), `phylo.niche.shift` assesses whether individual bioclimatic variables drift from their expected position. The basic idea is to simulate the bioclimatic variables at  $CC_{drift}$  under BM (which produces no drift) and then compare the simulated values to the real values. The algorithm works as follows. First, given the most recent common ancestor ( $CC_{mrca}$ ) of the species belonging to  $CC_{drift}$ , the function calculates the bioclimatic vector of ancestral state estimates at  $CC_{mrca}$  using both the `RRphylo` function (Castiglione et al. 2020) and the `phyEstimate` function in the R package `picante` (Kembel et al. 2010). With `phyEstimate`, we calculated the bioclimatic vector at  $CC_{mrca}$  according to BM, obtained via phylogenetic imputation (Garland & Ives 2000), assuming  $CC_{drift}$  is represented by a single species with unknown bioclimatic values. To be conservative, for each bioclimatic variable, the ancestral state estimate is chosen between `RRphylo` and `phyEstimate` valuations as the one closest to the mean value of the tips descending from  $CC_{mrca}$ . The resulting bioclimatic vector of estimates at  $CC_{mrca}$  is retained and set as the vector of phylogenetic means to simulate 100 new BM distributions of the variables on  $CC_{drift}$  proceeding with the Brownian rate  $\sigma^2$  calculated for the rest of the tree. A bioclimatic variable is deemed to drift if the mean of the real values falls outside 95% of the range of means generated by the 100 BM distributions.

### Simulating drifts in the position of the climatic niche as applied to a specific clade

To simulate a displacement in the average climatic niche position of a clade, we started sampling a  $d$  value within a family of 100 values ranging from 0.3 to 3. The scalar  $d$  was multiplied by the mean bioclimatic vector of the species belonging to the selected clade ( $y_0$ ) so as to produce a set of drifted bioclimatic variables. A three-fold change in  $y_0$  would, for instance, effectively transform a clade of warm-loving, Tropical species into high-latitude species experiencing cold temperatures, and *vice versa*

(e.g. a change from 5 to 15°C in mean annual temperature), covering most of the known climatic variability in Eurasia.

Overall, for each tree and each scenario, we produced a starting matrix of bioclimatic vectors,  $y$  (each row representing a species), a matrix where a shift in the rate is applied to a selected clade  $CC_{sel}$ ,  $yS$ , and a matrix where a drift is applied to  $CC_{sel}$ , named  $yD$ . We performed six different `phylo.niche.shift` runs, on  $y$  either non-indicating (automatic mode,  $y-auto$ ), or indicating the  $CC_{sel}$  (node mode,  $y-node$ ), the same on  $yS$  ( $yS-auto$  and  $yS-node$ ) and on  $yD$  ( $yD-auto$  and  $yD-node$ ).

To assess the power and sensitivity of `phylo.niche.shift` in finding rate shifts, we regressed the  $P$ -value produced by the function (which is two-tailed so that significance is accepted for either  $P < 0.025$  or  $P > 0.975$ ; at  $\alpha = 0.05$ ) on  $yS-node$  against the logarithm of the *effect* value, using logistic growth function in R. This approach correctly allows the gradual interpretation of  $P$ -values (Muff et al. 2021). The 'goodness-of-fit' of the logistic growth is approximated by calculating the model's Efron's pseudo- $R^2$  (Efron 1978), that is the squared correlation between the predicted and actual values. The  $P$ -values of *effect* predicted by the logistic model at  $P = 0.025$  and  $P = 0.975$ , represent the level of *effect* necessary to produce significant rate shifts as assessed by `phylo.niche.shift`. We further counted the percentage of shifts across the simulations on  $y-node$  and the Type I error on  $y-node$  at *effect* = 1 (see Appendix S1). The `phylo.niche.shift` function repeats, upon indication by the user, the rate shift test assuming the BM model of evolution. To this end, we used function `brownie.lite` in `phytools` (Revell 2012) which applies the noncensored approach described by O'Meara et al. (2006) to test for the existence of multiple rates on the tree. We replicated the assessment of false-positive incidence rate under BM to  $y-node$ .

To assess the power and sensitivity of `phylo.niche.shift` in finding climatic niche drifts, we counted the number of times the bioclimatic vector of  $CC_{sel}$  was found to drift in  $yD-node$  simulations and calculated the minimum  $d$  value necessary to provide significance at  $\alpha = 0.05$  for the simulations with both  $d > 1$  and  $d < 1$ . The number of times the bioclimatic vector of  $CC_{sel}$  was found to drift by using  $y-node$  provides the incidence of Type I errors. We further counted the average number of bioclimatic variables included in each simulation and those found to drift under both  $yS-node$  and  $y-node$ .

We estimated power and Type I error in finding shifts by using  $yD-node$  and in finding drifts by using  $yS-node$ , to assess how often applied rate shifts provide evidence

of drifts and vice versa, since the two are expected to influence each other (Saupe et al. 2019).

## Applying `phylo.niche.shift` to climatic niche evolution in primates

We collected 122950 occurrences belonging to 453 records of extant primate species. The occurrences were downloaded from the Global Biodiversity Information Facility online database (<https://www.gbif.org>). We excluded individual occurrences reported as 'preserved specimens' in the database, and corrected taxonomic and geographic errors, taking the International Union for Conservation of Nature's Red List and range maps as a reference. After this manipulation, the number of accepted occurrences reduced to 89269, and the number of valid species to 398. *Homo sapiens* was excluded from the tree because our climatic niche depends on technology, rather than physiology.

The phylogenetic tree is an informal supertree derived by integrating phylogenetic information from different sources (Appendix S1). We started from the phylogeny available in Melchionna et al. (2020) and updated it with missing species by means of the *tree.merger* function (Castiglione et al. 2022), embedded in *RRphylo*. Node ages for calibration were derived from TimeTree (Kumar et al. 2017), and adjusted according to known fossil information. The final tree and data included 365 extant species. We applied `phylo.niche.shift` to the primates' tree and data under the automatic mode, by setting the minimum size of the clades to be scanned for rate shift (*f*) at 15 species.

## RESULTS

### Virtual species' distributions: power and accuracy of `phylo.niche.shift` in detecting rate shifts in climatic niche evolution

The average tree size is 107.8 species. Both the latitudinal diversity and range-size gradients are reproduced in the data, indicating that virtual species' distributions conform to well-known macroecological patterns (Table 2). Under AE, the phylogenetic signal *K* in the bioclimatic variables distributions falls in the 0.41–0.71 range. Under RCE and CDE, the corresponding figures are 0.10–0.21 and 0.91–1.20, respectively, confirming our expectation that the signal grows from RCE towards CDE.

The logistic growth model provides very high Efron's *R*<sup>2</sup> for AE (0.982, Table 3; Fig. 2) and still large *R*<sup>2</sup> for both RCE and CDE (0.897 and 0.887, respectively, Table 3; Appendix S1 Figs. S1.2, S1.5). Despite the profound differences between the three scenarios, the significance levels

**Table 2.** The proportion of iterations where a significant negative latitudinal diversity gradient and significant positive latitudinal gradient in range size apply under each climatic evolution scenario (anticlimatic evolution – AE, random climate evolution – RCE, and climate-driven evolution – CDE). The average phylogenetic signal is calculated across all the selected bioclimatic variables when no rate shift is applied (*K<sub>y</sub>*), when the shift is applied to a specific clade (*K<sub>yS</sub>*), and when a drift in climatic niche position is applied to a specific clade (*K<sub>yD</sub>*)

	AE	RCE	CDE
Latitudinal diversity gradient	0.992	0.992	0.993
Latitudinal range size gradient	0.797	0.815	0.805
<i>K<sub>y</sub></i>	0.41 (0.37–0.66)	0.098 (0.09–0.12)	0.91 (0.79–1.5)
<i>K<sub>yS</sub></i>	0.42 (0.37–0.67)	0.098 (0.089–0.13)	0.87 (0.69–1.6)
<i>K<sub>yD</sub></i>	0.71 (0.49–1.2)	0.21 (0.12–0.46)	1.20 (0.89–2.3)

of *effect* are remarkably constant (Table 3), providing evidence that `phylo.niche.shift` is not very sensitive to the underlying mode of evolution of the climatic niche. The percentage of iterations where no shift is applied and yet a shift is returned is low under AE, reaches some 30% under RCE and reaches almost 100% under CDE. This properly reflects the finding that rate variation among *CC<sub>can</sub>* is much larger than would be expected under a single-rate (BM) model (Appendix S1). The incidence of Type I errors on *y*-node provided by `phylo.niche.shift` is low under all models (Table 3). By using *y-auto* under AE, 33% of the simulations showed at least one significant rate shift. However, large this figure could appear, it must be considered that the entire set of *CC<sub>can</sub>* is tested specifying automatic node. Since each tree contains

**Table 3.** The Efron pseudo-*R*<sup>2</sup> of the logistic regression between the simulated rate shift (*effect*) and the *P*-value returned by `phylo.niche.shift`. 'effect down' and 'effect up' indicate the *effect* value at which 95% of the `phylo.niche.shift` runs correctly identify the rate shift with a simulated decrease or increase, respectively. No shift is expected to occur at *effect* = 1. The last three rows report: (a) the proportions of rate shifts found across all simulation when no shift is simulated; (b) the same figure calculated assuming the Brownian motion model of climatic niche evolution; and (c) the figure when a drift, rather than a shift, is simulated. Anticlimatic evolution – AE, random climatic evolution – RCE, climate-driven evolution – CDE

	AE	RCE	CDE
Efron pseudo- <i>R</i> <sup>2</sup>	0.982	0.897	0.887
effect down	2.22	2.4	2.09
effect up	1.43	1.51	1.53
Type I error	0.003	0.071	0.082
a. Incidence of shifts found, <i>y</i> -node	0.044	0.299	0.976
b. Incidence of shifts found, BM, <i>y</i> -node	0.012	0.159	0.471
c. Incidence of shifts found, <i>yD</i> -node	0.66	0.797	0.805

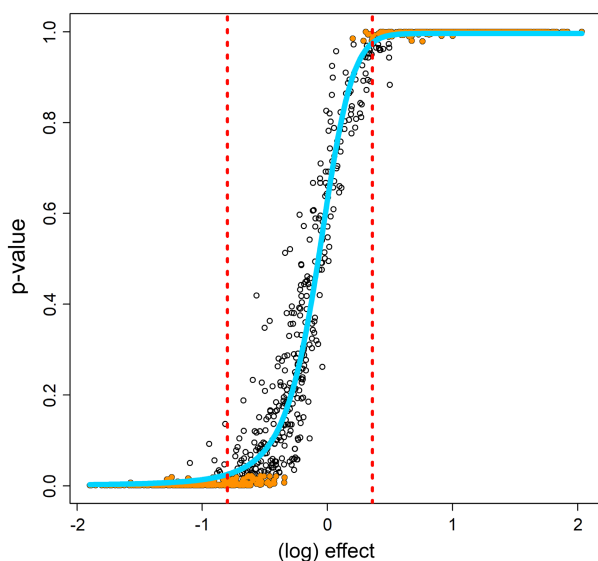


**Fig. 2.** Sensitivity of `phylo.niche.shift` to the simulated shifts in the rate of climatic niche evolution applied ( $y$ -axis) under the anticlimatic evolution scenario. Filled dots represent instances of significant results, for either instances of simulated rate decrease ( $P$ -value  $< 0.025$ ) or increase ( $P$ -value  $> 0.975$ ). The vertical dashed lines represent the values of the logarithm of the simulated effect where the fitted logistic curve ( $S$ -curve) reaches predicted  $P$ -values of 0.025 and 0.975.

12.2  $CC_{can}$  on average, the number of expected simulations finding at least one shift at  $\alpha = 0.05$  is 34% according to the binomial distribution, which confirms that the Type I error rate is below the  $\alpha$  nominal level. Under RCE, most of the iterations (92%) found at least one shifting clade by using  $y$ -auto.

With an incidence of rate shifts found at 0.159 (Table 3) and 12.2 clade in  $CC_{can}$  on average, the expected figure is 0.875. Finally, under CDE, the figure is higher still (96%) and this is to be explained by the very wide rate variation among  $CC_{can}$  clades under this scenario, that is two orders of magnitude larger than under BM (Appendix S1).

### Virtual species' distributions: power and accuracy of `phylo.niche.shift` in detecting drifts in climatic niche evolution

The application of a drift was successfully recognised by `phylo.niche.shift` in most cases. A mere change in the mean value of the selected variables by some 15% (Table 4; Appendix S1, Figs. S1.1, S1.3, S1.6), under all scenarios and whether a reduction or an increase in variables values is imposed by applying  $d$ , is sufficient to achieve significance. Type I error is extremely low under both AE and RCE (Table 4). In contrast, under RCE, the drift is common even without imposing a drift (Table 4).

The precision of `phylo.niche.shift` obtained using automatic mode is high. The clades set to drift corresponds to 95% of the clades found to drift by using  $yD$ -auto under AE, 95% of the clades are found to drift in RCE. Under CDE, the figure is much lower (57%), which must be explained by the wide rate variation intrinsic to  $CC_{can}$  with this scenario.

For the simulations where  $d$  was selected to be either above ' $d$  up' or below ' $d$  down' (Table 4), the number of bioclimatic variables found to drift under AE by using  $yD$ -auto is 3.8 times larger than with  $y$ -node (Table 4; Fig. 3). The same figure under RCE is 2.7 (Appendix S1, Fig. S1.4).

Under the last CDE scenario, the number of bioclimatic variables found to drift was as low as 50% of the total number of variables (Appendix S1, Fig. S1.7), a figure consistently lower than with AE (80%) and RCE (87%, Table 4). When using non-drifted bioclimatic vectors (i.e. with  $y$ -node), the number of bioclimatic variables found to drift is in the 21% to 32% range (Table 4).

### Climatic niche evolution in primates

By scanning the primate tree in search of climatic niche rate shifts, we found a negative shift pertaining to Strepsirrhini (rate difference =  $-37.76$ ,  $P$ -value  $< 0.001$ ).

**Table 4.** The percentage of drifts found as applied to the selected clade per different scenario when a drift is not applied ( $y$ -node), when it is applied ( $yD$ -node) and when a rate shift is applied ( $yS$ -node). ' $d$  down' and ' $d$  up' indicate the  $d$  value at which 95% of the `phylo.niche.shift` applications correctly identify the drift when a decrease or increase, respectively, in  $d$  is simulated. No drift is expected to occur at  $d = 1$ . Anticlimatic evolution – AE, random climatic evolution – RCE, climate-driven evolution – CDE

	AE	RCE	CDE
Incidence of drifts found, $y$ -node	0.003	0.008	0.413
Incidence of drifts found, $yS$ -node	0.366	0.406	0.55
Incidence of drifts found, $yD$ -node	0.85	0.843	0.897
$d$ down	0.84	0.84	0.87
$d$ up	1.17	1.18	1.08
Average length of bioclimatic vector	8.66	8.69	8.73
Average number of drifting bioclimatic variables, $y$ -node	1.841 (21.3%)	2.771 (31.8%)	2.194 (25.2%)
Average number of drifting bioclimatic variables, $yS$ -node	1.820 (21.0%)	2.812 (32.4%)	2.322 (26.7%)
Average number of drifting bioclimatic variables, $yD$ -node	6.942 (80.2%)	7.537 (86.7%)	4.456 (51.0%)

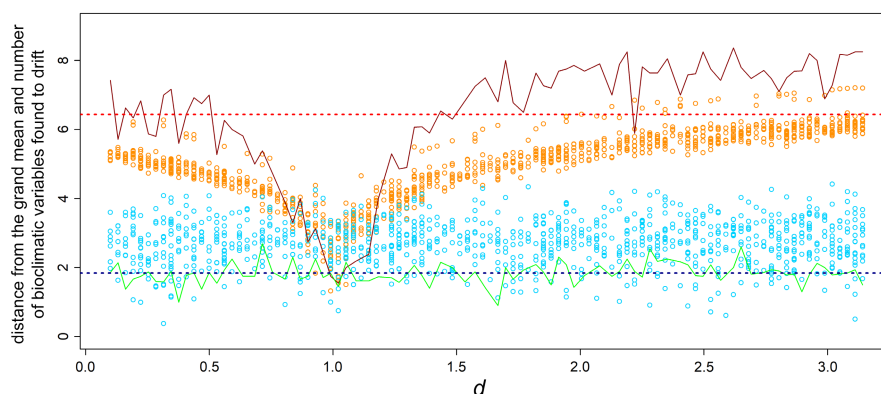


**Fig. 3.** The sensitivity of `phylo.niche.shift` to the intensity of the drift applied (x-axis), under the anticlimatic evolution scenario. On the y-axis, we report the logarithm of the Euclidean distance from the bioclimatic vector of means calculated over the entire tree, and the vector of means of the selected clade before (dots around the bottom dashed line) and after (dots forming the V-shaped distribution) multiplying the clade bioclimatic variables for a scalar  $d$ . Still on the y-axis, we also report the mean number of individual bioclimatic variables found to drift after (bottom dashed horizontal line) and before applying the  $d$  transform (top dashed horizontal line) vector of bioclimatic means. The broken solid lines connect the mean numbers of drifting bioclimatic variables calculated over 50 consecutive intervals in  $d$  after (top) and before (bottom) applying the  $d$  transform.

The clades including grey langurs and lutung (*Semnopithecus* and *Trachypithecus*) and capuchin monkeys (both robust and gracile, *Cebus* and *Sapajus*) both show significant and positive rate shifts (langurs+lutung: rate difference = 33.94,  $P$ -value = 0.998; capuchins: rate difference = 78.14,  $P$ -value = 1).

We found a significant niche drift in Catarrhini. Old World monkeys occupy more seasonal climates than other major primate clades, as testified by significantly higher than expected precipitation in the wettest month (BIO13), significantly lower than expected precipitation of the driest month (BIO14) and coldest quarter (BIO19), and low isothermality (BIO3). On the 365 species primate tree, `phylo.niche.shift` required 3.5s to run.

## DISCUSSION

Phylogenetic groups of species differ widely in their realised climatic niche. These differences may result from selective changes promoting niche widening or its converse (Aagesen et al. 2016, Velasco et al. 2018, Mondanaro et al. 2020, Frost et al. 2022), or be essentially neutral with regards to the fundamental niche (Bonetti & Wiens 2014, Boucher et al. 2014, Saupe et al. 2019). Whether or not the fundamental niche changes, identifying such differences has a huge impact on our understanding of species diversity patterns (Rolland & Salamin 2016, Olalla-Tárraga et al. 2017, Rolland et al. 2018) of the link existing between climatic niche breadth and extinction risk (Wiens et al. 2019, Taheri et al. 2021) and of how climate change is impacting extinction and will continue to do so (Hanson et al. 2020, Trisos et al. 2020). Key to appreciating how species face environmental variation is understanding

whether their climatic niche shifts (i.e. expands or retracts), drifts (i.e. moves along the niche dimension), or both. Although there is solid recognition that phylogenetic effects must be considered to understand these changes under a proper comparative context (Kellermann et al. 2012, Gutiérrez-Pesquera et al. 2016), most researchers just estimate the phylogenetic signal in bioclimatic variables, or rely on standard models of evolution such as BM (Münkemüller et al. 2015, Corro et al. 2021) or the Ornstein–Uhlenbeck process (Velasco et al. 2018, Frost et al. 2022). Yet, BM resides on assumptions that can be unrealistic for describing climatic niche evolution (Diniz-Filho et al. 2012, Kamilar & Cooper 2013), and even a significant signal does not indicate that the effect of shared ancestry on species' climatic niche is relevant (Freckleton & Jetz 2009, Cooper et al. 2011, Münkemüller et al. 2015). The Ornstein–Uhlenbeck process does not allow evolutionary rates to change across the tree, reducing to specified sets of purported evolutionary regimes.

We propose a new method to test for both niche shift and drift under a phylogenetically explicit scenario making no *a priori* assumptions about the rate and direction of niche evolution. The method, running under the R algorithm `phylo.niche.shift`, proved to be precise and very accurate, returning low Type I error rate and pervasively finding instances of rate shift (hence changes in the niche width) with 1.5-fold rate change (2.2-fold for rate decreases) and for drifts as low as ca. 15% displacement from the original niche position, regardless of the simulated scenario of niche evolution. `phylo.niche.shift` effectively finds 'global' drifts (i.e. those pertaining to the bioclimatic vectors as a whole) accurately and with very low error, although the incidence of false-positives among



individual variables is large, suggesting caution against emphasising drifts into individual variables within the niche. We found remarkably high incidence of drifts under simulated shifts, and vice versa. This was expected, because a positive shift stretches the sampled bioclimatic niche space of clades to otherwise unexplored values, and suggests that instances of drifts and shifts should be investigated at once.

A number of methods developed to test niche shifts use the entire climatic variation experienced by the species within its range to represent its niche, and contrast the sampled climate against the background climate. The consideration of background climatic variability provides better delineation of the species' preferred conditions than presence-only data (Hengl et al. 2009, Broennimann et al. 2012). We relied on presence-only data, further reducing the sampled climates to bioclimatic vectors of average values. However, there is no formal impairment in deriving the bioclimatic vectors otherwise (i.e. by considering absence/pseudo-absence data). Furthermore, whereas the focus of such methods is studying niche shifts at the species level, `phylo.niche.shift` compares clades rather than species and accounts for phylogenetic effects. We deem the approach presented here to be best suited for large-scale investigations testing macroevolutionary hypotheses about climatic niche evolution, such as whether a particular trait conferred greater environmental tolerance to a clade (e.g. C4 photosynthesis in grasses, Aagesen et al. 2016; or brown fat in mammals, Oelkrug et al. 2013); or whether niche width correlates with rates of taxonomic diversification (Rolland & Salamin 2016). Similarly, testing for climatic niche drifts with `phylo.niche.shift` means addressing whether trait evolution allows a clade to reside into a previously unexplored niche space (e.g. antifreeze proteins and life in Polar water fishes, Chen et al. 1997).

We addressed primate climatic niche evolution. We found that the clade including lutungs and the grey langur, and especially, the clade including capuchin monkeys proved to exploit unexpectedly large climatic niches. Gracile capuchins *Cebus* spp. are typical inhabitants of the wet and equable climates in the Amazon rainforest and forest savanna mosaic to the north (in the Roraima area). In contrast, robust capuchins *Sapajus* spp. occur in cooler, drier, and more seasonal climates such as the Cerrado (a tropical savanna) and Caatinga (a xeric shrubland). Capuchins split into a robust and a gracile clade at the end of the Miocene, and *Sapajus* later greatly differentiated during the Pleistocene cooling (Lynch Alfaro et al. 2012), originating the great environmental variation (Appendix S1, Fig. S1.9) we found (Cáceres et al. 2014). The dichotomy between lutungs and grey langurs is very similar to the relationship between *Cebus* and *Sapajus*. Langurs *Semnopithecus* spp. in particular, inhabit exceptionally diverse habitats (from

deserts to the Himalayas to dense forest habitats). Strong effect of habitat filtering (i.e. shared climatic preferences among species) is a common feature of strepsirrhine communities (Kamilar et al. 2014), testifying how narrow the climatic niche of strepsirrhine clades is compared with that of haplorrhine clades. Finally, the drift of Catarrhini as a whole is probably to be explained by their presence in highly seasonal climates in Eurasia, which is unparalleled by the other major primate clades. All these results indicate that `phylo.niche.shift` effectively found known, somewhat expected patterns of climatic niche change within primates.

In this study, we present a new R tool, `phylo.niche.shift`, meant to find instances of climatic niche shifts and drifts on phylogenetic trees. The tool proved exceptionally fast, accurate and sensible, under widely different scenarios of climatic niche evolution. `phylo.niche.shift` may help to improve research on niche evolution, as it allows users to find deviations from the expected niche among clades in the tree.

## ACKNOWLEDGEMENTS

We are grateful to Francesco Carotenuto for his advice on an early version of this manuscript. Open Access Funding provided by Università degli Studi di Napoli Federico II within the CRUI-CARE Agreement. Open Access Funding provided by Università degli Studi di Napoli Federico II within the CRUI-CARE Agreement.

## DATA AVAILABILITY STATEMENT

Data and R codes are available at [10.5281/zenodo.6143630](https://doi.org/10.5281/zenodo.6143630)

## REFERENCES

- Aagesen L, Biganzoli F, Bena J, Godoy-Bürki AC, Reinheimer R, Zuloaga FO (2016) Macro-climatic distribution limits show both niche expansion and niche specialization among C4Panicoideids. *PLoS One* 11: e0151075
- Blomberg SP, Garland T, Ives AR (2003) Testing for phylogenetic signal in comparative data: behavioral traits are more labile. *Evolution* 57: 717–745.
- Bonetti MF, Wiens JJ (2014) Evolution of climatic niche specialization: a phylogenetic analysis in amphibians. *Proceedings of the Royal Society B: Biological Sciences* 281: 20133229
- Boucher FC, Thuiller W, Davies TJ, Lavergne S (2014) Neutral biogeography and the evolution of climatic niches. *American Naturalist* 183: 573–584.
- Broennimann O, Fitzpatrick MC, Pearman PB, Petitpierre B, Pellissier L, Yoccoz NG et al. (2012) Measuring ecological niche overlap from occurrence and spatial

- environmental data. *Global Ecology and Biogeography* 21: 481–497.
- Cáceres N, Meloro C, Carotenuto F, Passaro F, Sponchiado J, Melo GL, Raia P (2014) Ecogeographical variation in skull shape of capuchin monkeys. *Journal of Biogeography* 41: 501–512.
- Castiglione S, Serio C, Mondanaro A, Melchionna M, Carotenuto F, Di Febbraro M, Profico A, Tamagnini D, Raia P (2020) Ancestral state estimation with phylogenetic ridge regression. *Evolutionary Biology* 47: 220–232.
- Castiglione S, Serio C, Mondanaro A, Melchionna M, Raia P (2022) Fast production of large, time-calibrated, informal supertrees with tree.merger. *Palaeontology* 65: e12588
- Castiglione S, Tesone G, Piccolo M, Melchionna M, Mondanaro A, Serio C, Di Febbraro M, Raia P (2018) A new method for testing evolutionary rate variation and shifts in phenotypic evolution. *Methods in Ecology and Evolution* 9: 974–983.
- Chen L, DeVries AL, Cheng C-HC (1997) Convergent evolution of antifreeze glycoproteins in Antarctic notothenioid fish and Arctic cod. *Proceedings of the National Academy of Sciences* 94: 3817–3822.
- Cooper N, Freckleton RP, Jetz W (2011) Phylogenetic conservatism of environmental niches in mammals. *Proceedings of the Royal Society B: Biological Sciences* 278: 2384–2391.
- Corro EJ, Villalobos F, Lira-Noriega A, Guevara R, Guimarães PR, Dáttilo W (2021) Annual precipitation predicts the phylogenetic signal in bat–fruit interaction networks across the Neotropics. *Biology Letters* 17: 20210478
- Diamond SE, Chick LD (2018) The Janus of macrophysiology: stronger effects of evolutionary history, but weaker effects of climate on upper thermal limits are reversed for lower thermal limits in ants. *Current Zoology* 64: 223–230.
- Diniz-Filho JAF, Santos T, Rangel TF, Bini LM (2012) A comparison of metrics for estimating phylogenetic signal under alternative evolutionary models. *Genetics and Molecular Biology* 35: 673–679.
- Efron B (1978) Regression and ANOVA with zero-one data: measures of residual variation. *Journal of the American Statistical Association* 73: 113–121.
- Fick SE, Hijmans RJ (2017) WorldClim 2: new 1-km spatial resolution climate surfaces for global land areas. *International Journal of Climatology* 37: 4302–4315.
- Freckleton RP (2009) The seven deadly sins of comparative analysis. *Journal of Evolutionary Biology* 22: 1367–1375.
- Freckleton RP, Jetz W (2009) Space versus phylogeny: disentangling phylogenetic and spatial signals in comparative data. *Proceedings of the Royal Society B: Biological Sciences* 276: 21–30.
- Frost L, Santamaria-Aguilar DA, Singletary D, Lagomarsino LP (2022) Neotropical niche evolution of *Otoba* trees in the context of global biogeography of the nutmeg family. *Journal of Biogeography* 49: 156–170.
- Garland T, Ives AR (2000) Using the past to predict the present: confidence intervals for regression equations in phylogenetic comparative methods. *American Naturalist* 155: 346–364.
- Gaston KJ, Blackburn TM (2007) *Pattern and Process in Macroecology*. Blackwell Publishing, Oxford, UK.
- Gutiérrez-Pesquera LM, Tejedo M, Olalla-Tárraga MÁ, Duarte H, Nicieza A, Solé M (2016) Testing the climate variability hypothesis in thermal tolerance limits of tropical and temperate tadpoles. *Journal of Biogeography* 43: 1166–1178.
- Hanson JO, Rhodes JR, Butchart SHM, Buchanan GM, Rondinini C, Ficetola GF, Fuller RA (2020) Global conservation of species' niches. *Nature* 580: 232–234.
- Hengl T, Sierdsema H, Radović A, Dilo A (2009) Spatial prediction of species' distributions from occurrence-only records: combining point pattern analysis, ENFA and regression-kriging. *Ecological Modelling* 220: 3499–3511.
- Holt RD, Gaines MS (1992) Analysis of adaptation in heterogeneous landscapes: implications for the evolution of fundamental niches. *Evolutionary Ecology* 6: 433–447.
- Kamilar JM, Beaudrot L, Reed KE (2014) The influences of species richness and climate on the phylogenetic structure of African haplorhine and strepsirrhine primate communities. *International Journal of Primatology* 35: 1105–1121.
- Kamilar JM, Cooper N (2013) Phylogenetic signal in primate behaviour, ecology and life history. *Philosophical Transactions of the Royal Society B: Biological Sciences* 368: rstb.2012.0341
- Kellermann V, Loeschcke V, Hoffmann AA, Kristensen TN, Fløjgaard C, David JR, Svenning JC, Overgaard J (2012) Phylogenetic constraints in key functional traits behind species' climate niches: patterns of desiccation and cold resistance across 95 *Drosophila* species. *Evolution* 66: 3377–3389.
- Kemmel SW, Cowan PD, Helmus MR, Cornwell WK, Morlon H, Ackerly DD, Blomberg SP, Webb CO (2010) Picante: R tools for integrating phylogenies and ecology. *Bioinformatics* 26: 1463–1464.
- Kozak KH, Wiens JJ (2010) Accelerated rates of climatic-niche evolution underlie rapid species diversification. *Ecology Letters* 13: 1378–1389.
- Kumar S, Stecher G, Suleski M, Hedges SB (2017) TimeTree: a resource for timelines, timetrees, and divergence times. *Molecular Biology and Evolution* 34: 1812–1819.
- Lancaster LT, Humphreys AM (2020) Global variation in the thermal tolerances of plants. *Proceedings of the*

- National Academy of Sciences of the United States of America* 117: 13580–13587.
- Lynch Alfaro JW, Boubli JP, Olson LE, Di Fiore A, Wilson B, Gutiérrez-Espeleta GA et al. (2012) Explosive Pleistocene range expansion leads to widespread Amazonian sympatry between robust and gracile capuchin monkeys. *Journal of Biogeography* 39: 272–288.
- Melchionna M, Mondanaro A, Serio C, Castiglione S, Di Febbraro M, Rook L et al. (2020) Macroevolutionary trends of brain mass in primates. *Biological Journal of the Linnean Society* 129: 14–25.
- Mondanaro A, Melchionna M, Di Febbraro M, Castiglione S, Holden PB, Edwards NR et al. (2020) A major change in rate of climate niche envelope evolution during hominid history. *iScience* 23: 101693.
- Muff S, Nilsen EB, O'Hara RB, Nater CR (2021) Rewriting results sections in the language of evidence. *Trends in Ecology & Evolution* 37: 203–210.
- Münkemüller T, Boucher FC, Thuiller W, Lavergne S (2015) Phylogenetic niche conservatism – common pitfalls and ways forward. *Functional Ecology* 29: 627–639.
- Oelkrug R, Goetze N, Exner C, Lee Y, Ganjam GK, Kutschke M et al. (2013) Brown fat in a protoendothermic mammal fuels eutherian evolution. *Nature Communications* 4: 1–8.
- Olalla-Tárraga MÁ, González-Suárez M, Bernardo-Madrid R, Revilla E, Villalobos F (2017) Contrasting evidence of phylogenetic trophic niche conservatism in mammals worldwide. *Journal of Biogeography* 44: 99–110.
- O'Meara BC, Ané C, Sanderson MJ, Wainwright PC (2006) Testing for different rates of continuous trait evolution using likelihood. *Evolution* 60: 922–933.
- Perez TM, Feeley KJ (2021) Weak phylogenetic and climatic signals in plant heat tolerance. *Journal of Biogeography* 48: 91–100.
- Revell LJ (2012) phytools: An R package for phylogenetic comparative biology (and other things). *Methods in Ecology and Evolution* 3: 217–223.
- Revell LJ, Harmon LJ (2008) Testing quantitative genetic hypotheses about the evolutionary rate matrix for continuous characters. *Evolutionary Ecology Research* 10: 311–331.
- Rolland J, Salamin N (2016) Niche width impacts vertebrate diversification. *Global Ecology and Biogeography* 25: 1252–1263.
- Rolland J, Silvestro D, Schluter D, Guisan A, Broennimann O, Salamin N (2018) The impact of endothermy on the climatic niche evolution and the distribution of vertebrate diversity. *Nature Ecology and Evolution* 2: 459–464.
- Saupe EE, Myers CE, Peterson AT, Soberón J, Singarayer J, Valdes P, Qiao H (2019) Non-random latitudinal gradients in range size and niche breadth predicted by spatial patterns of climate. *Global Ecology and Biogeography* 28: 928–942.
- Song G, Li Y, Zhang J, Li M, Hou J, He N (2016) Significant phylogenetic signal and climate-related trends in leaf caloric value from Tropical to cold-Temperate forests. *Scientific Reports* 6: 1–10.
- Taheri S, Naimi B, Rahbek C, Araújo MB (2021) Improvements in reports of species redistribution under climate change are required. *Science Advances* 7: 1–12.
- Trisos CH, Merow C, Pigot AL (2020) The projected timing of abrupt ecological disruption from climate change. *Nature* 580: 496–501.
- Velasco JA, Martínez-Meyer E, Flores-Villela O (2018) Climatic niche dynamics and its role in the insular endemism of *Anolis* lizards. *Evolutionary Biology* 45: 345–357.
- Wiens JJ, Litvinenko Y, Harris L, Jezkova T (2019) Rapid niche shifts in introduced species can be a million times faster than changes among native species and ten times faster than climate change. *Journal of Biogeography* 46: 2115–2125.
- Zuur AF, Ieno EN, Elphick CS (2010) A protocol for data exploration to avoid common statistical problems. *Methods in Ecology and Evolution* 1: 3–14.

## SUPPORTING INFORMATION

Additional supporting information may be found in the online version of this article at the publisher's website.

**Appendix S1.** Supplementary methods.